

QSAR and Molecular Docking of Pyrimidine Derivatives Against *Plasmodium falciparum* dihydrofolate reductase-thymidylate synthase (PfDHFR-TS)

Putra Jiwamurwa Pama TJITDA^{1*} , Febri Odel NITBANI² , Dominus MBUNGA¹ 

¹ Department of Pharmacy, Health Polytechnic of Kupang, Kupang, Indonesia

² Department of Chemistry, Faculty of Science and Engineering, University of Nusa Cendana, Kupang, Indonesia

* Corresponding Author. E-mail: putratjitda@poltekkeskupang.ac.id (P.J.P.T.); Tel. +62-812-373 03 590.

Received: 04 January 2022 / Revised: 10 June 2022 / Accepted: 10 June 2022

ABSTRACT: New pyrimidine compounds were developed using quantitative structure-activity relationship (QSAR) analysis and molecular docking. The aim of the research was to find the best QSAR equation and to investigate the interaction of the new compound with the target protein of dihydrofolate reductase thymidylate synthase of *P. falciparum* by molecular docking. Each compound was optimized using AM1 computational methods. In QSAR analysis, statistical calculations involving multi-linear regression (MLR) were performed. The results of QSAR analysis yielded the best equation model, namely $\text{Log pMIC} = 10.441 - 16.769 (\text{qC7}) - 15.880 (\text{qC9}) + 5.809 (\text{qC12}) + 10.612 (\text{qC13}) + 114.506 (\text{LUMO})$. The addition of electron donating groups such as hydroxyl, amino, N,N-dimethyl amine and halogen also enhanced the antimalarial activity. The molecular docking results showed that the new design of pyrimidine compounds is able to interact with important amino acid residues on the target protein via hydrogen bonds. The presence of pyrrolidine on the C3 pyrimidine ring contributed to the interaction with key amino acid residues via hydrophobic interactions.

KEYWORDS: Pyrimidine; QSAR; Molecular Docking; Antimalarial.

1. INTRODUCTION

Malaria is a disease caused by the *Anopheles mosquito's* transmission and several groups of plasmodium such as *Plasmodium falciparum* and *Plasmodium vivax* [1], which could destroy erythrocytes. In 2019, epidemiological studies found that malaria caused 409 deaths out of 229 million cases [2]. The spread of this disease is mostly found in tropical countries such as Africa, the eastern Mediterranean, and about 3.5% are spread throughout South Asian Countries [3]. In Indonesia, several areas such as Papua, West Papua, Maluku, North Maluku, and East Nusa Tenggara are classified as malaria-endemic areas [2]. Malaria is a dangerous disease because it could be fatal for the sufferer. Children and pregnant women have a higher risk factor of death if they suffer from this disease [4].

Many efforts to reduce malarial diseases have been carried out through antimalarial drug treatments such as chloroquine, primaquine, or mefloquine. However, along with the implementation of the therapy, it causes parasite mutations leading to antimalarial drug resistance [5]. Therefore, this prompted a study to find new drugs expected to have higher effectiveness in malaria therapeutic.

Pyrimidine compounds are a group of heterocyclic compounds containing six rings and two nitrogen atoms. Pyrimidine derivatives have broad biological activity Kalaria et al. [6] reported that pyrimidine derivative compounds had good antimalarial activity. Agarwal et al. [7] had succeeded in synthesizing derivatives of 2,4,6-trisubstituted pyrimidine compounds and these compounds showed potential activity as antimalarials. The results showed that as many as 18 synthetic compounds were able to fight *Plasmodium falciparum* NF-54 strain cultures and had MIC values in the range of 0.25-2 g/mL. Pyrimidine derivatives had also been successfully synthesized and proven to be able to fight several strains of malaria agents such as *Plasmodium berghei* [8], *Plasmodium falciparum* W2 strain [9], and *Plasmodium falciparum* D6 strain [10].

The study of potential drug discovery as an antimalarial agent continues to develop over the years. Research in the laboratory through a series of synthesis reaction schemes and purification of compounds has

How to cite this article: Tjitda, PJP, Nitbani, FO, Mbunga, D. QSAR and Molecular Docking of Pyrimidine Derivatives Against *Plasmodium falciparum* dihydrofolate reductase-thymidylate synthase (PfDHFR-TS). J Res Pharm. 2022; 26(6): 1723-1735.

been carried out. However, these procedures are time-consuming, costly, and produce waste that is harmful to the environment [11]. Computer-Aided Drug Design (CADD) is a promising computational study because it could increase the efficiency of drug discovery [12]. This method offers the modification structure by following the descriptor data, using statistical principles, and correlating the structural properties of the compounds with their biological activities. Quantitative Structure-Activity Relationship (QSAR) has become a solution in drug discovery because the modified compound obtained has better therapeutic activities [13]. Based on the literature study, the QSAR study of pyrimidine derivative compounds have not yet been carried out.

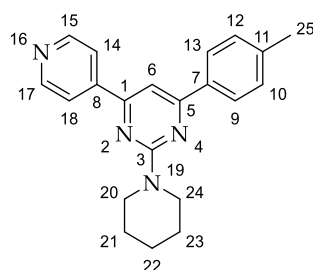
In this research, a QSAR study was performed on several series of 2,4,6-trisubstituted pyrimidine derivatives using the data from the synthesized compound by Agarwal et al [7]. The new design compound from QSAR study was docked to *Plasmodium falciparum* dihydrofolate reductase-thymidylate synthase (*Pf*-DHFR-TS) to evaluate the interaction and binding energy by molecular docking. *Pf*DHFR-TS enzyme is an important enzyme in antimalarial drug discovery, which plays a role in the production of folate and thymidylate for DNA biosynthesis [14]. The crystal structure of the protein was taken from the PDB database with ID: 1J31. The crystal structure of *Pf*DHFR-TS contains the inhibitor WR99210, which effectively inhibits the enzyme dihydrofolate reductase, resulting in the failure of pyrimidine synthesis in *Plasmodium* and impaired folate metabolism [15].

2. RESULTS and DISCUSSION

2.1. QSAR Analysis

Firstly, the validation of optimization methods was conducted on the 3D structure of the pyrimidine compound. At this stage, the structure of compound 15 was optimized using several computational methods, namely AM1, PM3, HF, and DFT. To select the best computational method, the smallest PRESS is an indicator that the obtained chemical shift value calculated has similar to experiment ¹³C-NMR [16]. Table 1 shows the results of calculating the ¹³C-NMR chemical shift from several computational methods. The smallest PRESS value was represented by the AM1 method. Therefore, the AM1 method was the best method for calculating the atomic charge, HOMO, and LUMO values. This value is used as a descriptor in the QSAR analysis.

Table 1. ¹³C-NMR chemical shift calculation data for computational and experimental calculations.



Position	δ				
	experiment (ppm)	AM1	PM3	HF	DFT
C25	21.80	22.64	19.35	17.22	19.25
C22	25.40	24.27	22.46	19.41	21.74
C21 & C23	26.30	24.84	22.92	20.33	22.77
C20, C24	45.30	43.12	42.11	35.18	37.79
C6	101.40	101.15	90.46	88.29	89.71
C14 & C18	121.50	109.58	105.16	104.35	106.37
C9 & C13	127.40	113.04	109.99	109.28	111.70
C10, C12	129.80	113.74	113.22	110.83	113.23
C11	135.60	121.93	122.67	121.31	124.77
C7	141.20	119.31	113.60	116.27	117.83
C8	145.30	127.42	121.32	124.25	125.54
C15 & C17	150.80	133.89	134.04	128.39	133.26
C5	162.60	149.22	142.90	141.36	144.32
C3	162.90	155.57	150.50	134.62	141.00
C1	166.20	147.29	141.40	139.96	142.50
PRESS		2477.32	224762.33	224762.33	224762.33

The resulting descriptor that used as the dependent variable to build the QSAR equation. While the experimental MIC value was converted to the pMIC value and used as the independent variable. The experimental data (Table 6) were divided into two groups randomly. The first group is the training data as the building of the QSAR equation. On the other hand, the data set was executed to validate the QSAR equation. Multilinear regression (MLR) analysis using the backward method was performed to construct the QSAR equation. In the backward method, the significant level of the difference for each regression model produced was the F_{cal} value compared to F_{table} with a significance value of 0.05. The calculation of partial F_{cal} which had a small value to F_{table} was discarded and continued until the MLR calculation process had a high F_{cal}/F_{table} ratio. The obtained QSAR equation model is shown in Table 2.

Table 2. QSAR equation model analyzed by MLR.

Model	Descriptor	R	R ²	Adjusted R ²	SEE	F _{cal} /F _{table}	PRESS
1	qC3, qC7, qC9, qC10, qC12, qC13, LUMO	0.921	0.848	0.670	0.289	1.133	0.499
2	qC3, qC7, qC9, qC12, qC13, LUMO	0.895	0.801	0.630	0.306	1.212	0.654
3	qC7, qC9, qC12, qC13, LUMO	0.851	0.724	0.552	0.336	1.139	0.904

Table 3. Data on the difference between predicted pMIC and experimental pMIC is represented by the four QSAR equation models.

Compounds test	Experimental pMIC	Calculation of the predicted pMIC		
		Model 1	Model 2	Model 3
3	8.559	8.457	8.539	8.358
9	8.225	7.545	7.669	7.768
17	7.537	8.074	8.156	8.049
5	6.895	6.773	6.826	7.131
	PRESS	0.777	0.697	0.569

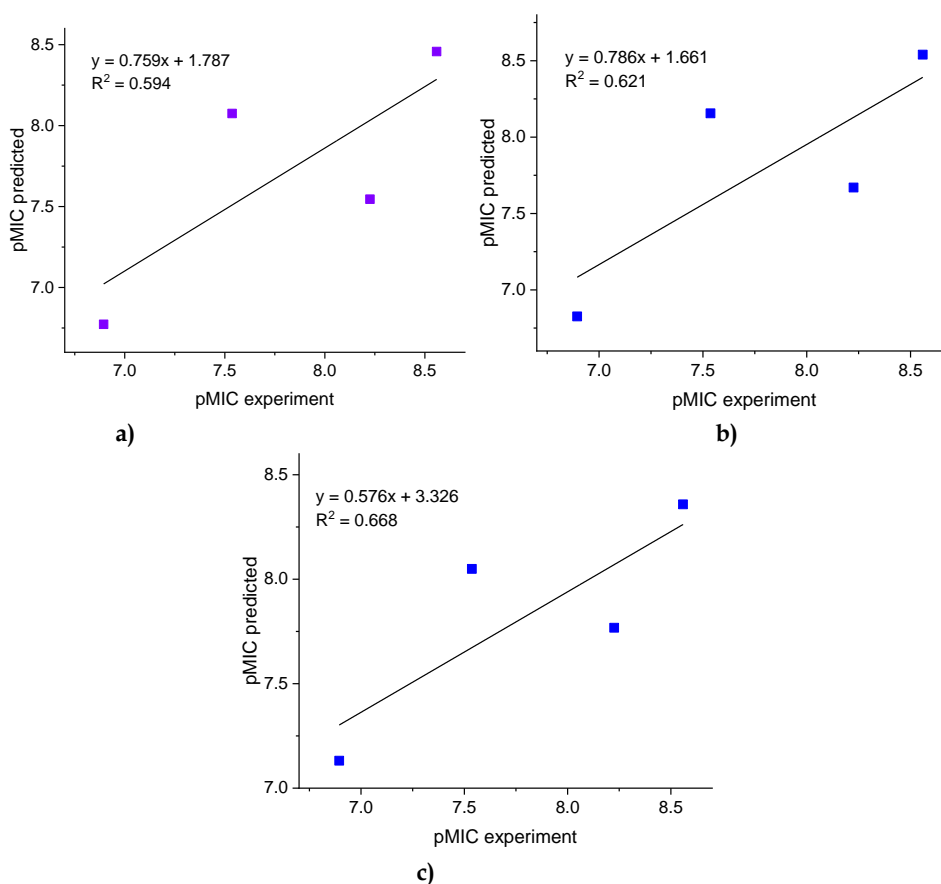


Figure 1. The plot of predicted pMIC versus experimental pMIC. model 1 (a), model 2 (b), and model 3 (c).

The MLR analysis of the obtained descriptors resulted in 3 models of the QSAR equation. The selected QSAR equation model based on statistics was performed. The correlation coefficient (R) value for the three equations ranged from 0.85 to 0.92. The R-value closest to 1 described the used descriptor that had to reflect the activity of the relationship. The other criteria were the R² value. This value shows that the relationship between the parameters used for antimalarial activity was quite good, with a range of 72-84% [17]. The selection of the best equation model was not only the two criteria. Moreover, it was also difficult to get the best equation model based on its standard error estimation (SEE) and PRESS of the three equation models. The three equation models gave a low score. The low value of SEE means that the obtained equation model had good accuracy on antimalarial activity. Furthermore, the PRESS value presents an adequately small value (<1). The smallest PRESS indicated that the obtained equation was close to the experimental value.

Selection of the best QSAR equation model from these criteria would be more difficult. Therefore, all three equation models were validated. The validation of the three equation models was carried out by measuring the predicted pMIC activity values using the test data set (Table 3). The values of R² and PRESS determine the best equation model that could be used to design new compounds. The R² value of the three equations yielded a fairly good result (Figure 1). However, model 3 gave a fairly good R² value, which was 0.688 [18]. Based on this value, the suggestion model is model 3 which has the closest value to the actual antimalarial activity. In addition, the PRESS value in model 3 had the lowest value. The lowest PRESS value confirmed that model 3 could be used as an equation model to design new pyrimidine compounds.

$$\text{(eq.1) } \log \text{pMIC} = 10.441 - 16.769(\text{qC7}) - 15.880(\text{qC9}) + 5.809(\text{qC12}) + 10.612(\text{qC13}) + 114.506(\text{LUMO})$$

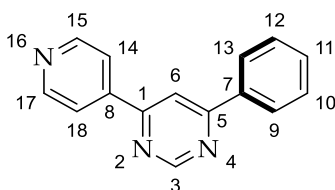
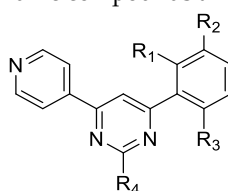


Figure 2. Structure of pyrimidine.

Model 3 had several descriptors that affect antimalarial activity. Model 3 could also be used as a guide for designing new pyrimidine compounds. At C7, this substitute could not be added because of the quaternary carbon. Meanwhile, C9, C12, and C13 were part of the core structure of pyrimidine compounds to which new substitutes could be added (bold mark in Figure 2). To obtain the best activity compound, we introduced some substitutes to decrease the MIC values (larger log pMIC values). It could be achieved by inserting an electron-donating group on C13 that caused the charge on C13 to become more positive and on the other hand, the charge on C7 became negative. The insertion of an electron-donating group at C13 also gave the pMIC value became more positive. Similar to C7, a negative charge on C7 was also generated by inserting an electron-donating or halogen group on C9. It caused the charge on C9 to be positive so that the charge on C7 became negative.

The lowest unoccupied molecular orbital (LUMO) also affects the activity of pyrimidine compounds. The LUMO value affects the reactivity of an aromatic ring. It describes the ability of the organic compounds to accept electrons and is associated with electron affinity (EA) [19]. The insertion of an electron donation group gave a smaller LUMO value. It leads to a low ionization potential (IP) and creates the nucleophilic properties of the aromatic ring [20]. Consequently, it might increase the antimalarial activity of the novel pyrimidine compounds. In this study, pyrimidine compounds were modified by inserting several new groups at positions R1, R2, and R3 based on the instruction of the selected QSAR equation. In addition, modification of the C3 pyrimidine ring with piperidine and pyrrolidine reported by Agarwal et al [7] showed good inhibitory activity against *Plasmodium falciparum*. However, these results could not provide clear information about the best group that contribute to this activity. Therefore, we also studied the effect of piperidine and pyrrolidine on antimalarial activity according to the QSAR equation, and for comparison, we also inserted the primary amino group.

Table 4. New design of pyrimidine compounds and their predicted pMIC values.



Compound id	R ₁	R ₂	R ₃	R ₄	pMIC Prediction
19	-OH	-H	-OH	-NH ₂	9.388
19a	-OH	-H	-OH	Piperidine	9.997
19b	-OH	-H	-OH	Pyrrolidine	10.249
20	-NH ₂	-H	-OH	-NH ₂	10.359
20a	-NH ₂	-H	-OH	Piperidine	10.487
20b	-NH ₂	-H	-OH	Pyrrolidine	10.411
21	-NH ₂	-H	-NH ₂	-NH ₂	10.542
21a	-NH ₂	-H	-NH ₂	Piperidine	9.564
21b	-NH ₂	-H	-NH ₂	Pyrrolidine	10.944
22	-NH ₂	-NH ₂	-NH ₂	-NH ₂	10.629
22a	-NH ₂	-NH ₂	-NH ₂	Piperidine	10.777
22b	-NH ₂	-NH ₂	-NH ₂	Pyrrolidine	10.988
23	-NH ₂	-N(CH ₃) ₂	-NH ₂	-NH ₂	10.925
23a	-NH ₂	-N(CH ₃) ₂	-NH ₂	Piperidine	10.107
23b	-NH ₂	-N(CH ₃) ₂	-NH ₂	Pyrrolidine	11.308
24	-NH ₂	-N(CH ₃) ₂	-F	-NH ₂	11.513
24a	-NH ₂	-N(CH ₃) ₂	-F	Piperidine	11.594
24b	-NH ₂	-N(CH ₃) ₂	-F	Pyrrolidine	11.080
25	-NH ₂	-N(CH ₃) ₂	-Cl	-NH ₂	12.227
25a	-NH ₂	-N(CH ₃) ₂	-Cl	Piperidine	12.477
25b	-NH ₂	-N(CH ₃) ₂	-Cl	Pyrrolidine	12.577
26	-NH ₂	-N(CH ₃) ₂	-Br	-NH ₂	13.494
26a	-NH ₂	-N(CH ₃) ₂	-Br	Piperidine	13.768
26b	-NH ₂	-N(CH ₃) ₂	-Br	Pyrrolidine	13.871
27	-NH ₂	-N(CH ₃) ₂	-I	-NH ₂	14.139
27a	-NH ₂	-N(CH ₃) ₂	-I	Piperidine	14.449
27b	-NH ₂	-N(CH ₃) ₂	-I	Pyrrolidine	14.788

Table 4 shows that several donating groups such as hydroxyl, amino, and N,N-dimethyl amine contributed to the antimalarial activity of the new compound pyrimidine. The addition of the halogen substituent on the R₃ position of the pyrimidine compounds was interesting to explain. In general, the insertion of the halogen substituent gave a good antimalarial activity. However, the change of the fluoro (-F) substituent to iodo (-I) gave an activity trend where it produced a higher pMIC value. According to this change, it decreased the electronegativity character, therefore its lone pair electron was easily donated to the aromatic ring. As a result, lower LUMO values and better antimalarial activity. In addition, the insertion of a pyrrolidine group at C3 of the pyrimidine ring generally showed better pMIC values. It was suspected that the insertion of pyrrolidine could reduce the energy value of LUMO, therefore the pMIC value was increased and the predictive antimalarial activity was better.

2.2. Molecular Docking

The design of the new compounds of pyrimidine had been carried out using by QSAR equation model guide. The resulting new compounds were then docked to the *Plasmodium falciparum* dihydrofolate reductase-thymidylate synthase protein. This protein structure (ID PDB: 1J3i) was retrieved from the RSCB website. Prior to molecular docking of new compound designs, re-docking was carried out to ensure the validity of the docking protocol. Re-docking of WR99210 as a native ligand against *Pf*DHFR-TS protein gave an RMSD value of 0.858 Armstrong (Figure 3). Molecular docking provides an overview of how the interaction of new compounds with the amino residue could predict the amount of binding energy between ligands (new pyrimidine compounds) on proteins. A total of 27 new compounds had been designed next to

the structure optimization with the AM1 method. Further, the molecular docking of the newly designed compound on the protein was worked and its results were shown in Table 5. The WR99210 is a potential inhibitor protein as an antimalarial compound and it could be a comparison of antimalarial activity toward newly designed compounds.

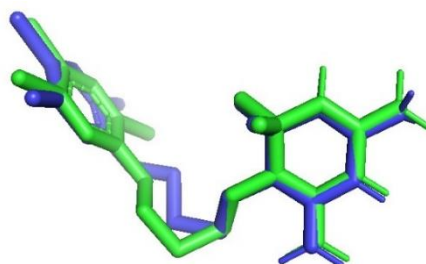


Figure 3. The protocol docking validation of *Pf*DHFR-TS protein (ID: 1j3i); green (native ligand) and blue (re-docking ligand).

Table 5. Binding energy, type, and distance interaction of new pyrimidine derivative compounds.

Compound	IUPAC name	Binding interaction	Distance interaction of hydrogen bond (Amstrong)	Binding energy (kcal/mol)
WR99210	6,6-dimethyl-1-[3-(2,4,5-trichlorophenoxy)propoxy]-1,6-dihydro-1,3,5-triazine-2,4-diamine	Ile14 (H-Bond), Cys15 (H-Bond), Asp54 (H-Bond), Ile164 (H-Bond), Phe116 (Halogen), Lys49 (Halogen)	2.10, 2.88, 2.05, 2.06	-8.9
19	2-(2-amino-6-(pyridin-4-yl)pyrimidin-4-yl)benzene-1,3-diol	Asp54 (H-Bond), Ser111 (H-Bond), Ile164 (H-Bond), Tyr170 (H-Bond)	2.15, 2.47, 2.13, 3.19	-8.2
19a	2-(2-(piperidin-1-yl)-6-(pyridin-4-yl)pyrimidin-4-yl)benzene-1,3-diol	Ile14, Asp54		-8.5
19b	2-(6-(pyridin-4-yl)-2-(pyrrolidin-1-yl)pyrimidin-4-yl)benzene-1,3-diol	Phe116		-8.3
20	3-amino-2-(2-amino-6-(pyridin-4-yl)pyrimidin-4-yl)phenol	Val45 (H-Bond), Tyr170 (H-Bond)	2.90, 2.45	-8.0
20a	3-amino-2-(2-(piperidin-1-yl)-6-(pyridin-4-yl)pyrimidin-4-yl)phenol	Ile14, Asp54 (H-Bond), Ile164 (H-Bond)	2.24, 2.42	-8.4
20b	3-amino-2-(6-(pyridin-4-yl)-2-(pyrrolidin-1-yl)pyrimidin-4-yl)phenol	Asp54 (H-Bond), Ile164 (H-Bond), Phe116	2.29, 2.20,	-8.2
21	2-(2-amino-6-(pyridin-4-yl)pyrimidin-4-yl)benzene-1,3-diamine	Ile14 (H-Bond), Val45 (H-Bond), Ile164 (H-Bond), Tyr170 (H-Bond)	2.01, 3.04, 1.98, 2.18	-8.0
21a	2-(2-(piperidin-1-yl)-6-(pyridin-4-yl)pyrimidin-4-yl)benzene-1,3-diamine	Ile14, Asp54 (H-Bond), Ile164 (H-Bond)	2.28, 2.39,	-8.4
21b	2-(6-(pyridin-4-yl)-2-(pyrrolidin-1-yl)pyrimidin-4-yl)benzene-1,3-diamine	Asp54 (H-Bond), Ile164 (H-Bond), Phe116 (Halogen)	2.29, 2.24	-8.5
22	3-(2-amino-6-(pyridin-4-yl)pyrimidin-4-yl)benzene-1,2,4-triamine	Ile14, Asp54, Ile164, Tyr170	1.95, 2.36, 1.90, 2.44	-8.6
22a	3-(2-(piperidin-1-yl)-6-(pyridin-4-yl)pyrimidin-4-yl)benzene-1,2,4-triamine	Ile14 (H-Bond), Asp54 (H-Bond), Ile164 (H-Bond)	2.56, 2.94, 2.04	-8.0
22b	3-(6-(pyridin-4-yl)-2-(pyrrolidin-1-yl)pyrimidin-4-yl)benzene-1,2,4-triamine	Ile14 (H-Bond), Asp54 (H-Bond), Ile164 (H-Bond), Phe116	2.14, 2.85, 1.93,	-8.9
23	3-(2-amino-6-(pyridin-4-yl)pyrimidin-4-yl)-N1,N1-dimethylbenzene-1,2,4-triamine	Ser108 (H-Bond), Ser111 (H-Bond)	2.68, 2.44	-8.2
23a	N1,N1-dimethyl-3-(2-(piperidin-1-yl)-6-(pyridin-4-yl)pyrimidin-4-yl)benzene-1,2,4-triamine	Asp54 (H-Bond), Phe116, Lys49 (H-Bond)	3.24, 3.31	-7.9
23b	N1,N1-dimethyl-3-(6-(pyridin-4-yl)-2-	Phe116		-8.2

24	(pyrrolidin-1-yl)pyrimidin-4-yl)benzene-1,2,4-triamine 3-(2-amino-6-(pyridin-4-yl)pyrimidin-4-yl)-4-fluoro-N1,N1-dimethylbenzene-1,2-diamine	-	-	-8.4
24a	4-fluoro-N1,N1-dimethyl-3-(2-(piperidin-1-yl)-6-(pyridin-4-yl)pyrimidin-4-yl)benzene-1,2-diamine	Ile14, Asp54 (H-Bond), Ile164 (H-Bond), Phe116	3.14, 3.31	-7.8
24b	4-fluoro-N1,N1-dimethyl-3-(6-(pyridin-4-yl)-2-(pyrrolidin-1-yl)pyrimidin-4-yl)benzene-1,2-diamine	Cys15, Phe116		-8.0
25	3-(2-amino-6-(pyridin-4-yl)pyrimidin-4-yl)-4-chloro-N1,N1-dimethylbenzene-1,2-diamine	Ser108 (H-Bond), Ser111 (H-Bond)	2.11, 2.42	-8.3
25a	4-chloro-N1,N1-dimethyl-3-(2-(piperidin-1-yl)-6-(pyridin-4-yl)pyrimidin-4-yl)benzene-1,2-diamine	-		-7.7
25b	4-chloro-N1,N1-dimethyl-3-(6-(pyridin-4-yl)-2-(pyrrolidin-1-yl)pyrimidin-4-yl)benzene-1,2-diamine	Cys15, Phe116		-7.9
26	3-(2-amino-6-(pyridin-4-yl)pyrimidin-4-yl)-4-bromo-N1,N1-dimethylbenzene-1,2-diamine	Ile164 (H-Bond), Leu40 (Halogen)	2.44	-8.2
26a	4-bromo-N1,N1-dimethyl-3-(2-(piperidin-1-yl)-6-(pyridin-4-yl)pyrimidin-4-yl)benzene-1,2-diamine	Asp54 (Halogen), Ile164 (H-Bond)	3.46	-7.6
26b	4-bromo-N1,N1-dimethyl-3-(6-(pyridin-4-yl)-2-(pyrrolidin-1-yl)pyrimidin-4-yl)benzene-1,2-diamine	Asp54 (H-Bond), Ile164 (Halogen), Phe116, Lys49 (H-Bond)	3.47, 3.41	-8.3
27	3-(2-amino-6-(pyridin-4-yl)pyrimidin-4-yl)-4-iodo-N1,N1-dimethylbenzene-1,2-diamine	Ile164 (H-Bond), Ser167 (Halogen)	2.53	-8.2
27a	4-iodo-N1,N1-dimethyl-3-(2-(piperidin-1-yl)-6-(pyridin-4-yl)pyrimidin-4-yl)benzene-1,2-diamine	Asp54 (Halogen), Ile164 (H-Bond)	3.60	-7.7
27b	4-iodo-N1,N1-dimethyl-3-(6-(pyridin-4-yl)-2-(pyrrolidin-1-yl)pyrimidin-4-yl)benzene-1,2-diamine	Ile164 (Halogen), Phe116, Lys49 (H-Bond)	3.35	-7.5

The results of molecular docking analysis informed that all new compounds had fairly good antimalarial activity. It was confirmed by their binding energy which was in the range of 7.5 to 8.9 kcal/mol. The new substituent on the compound facilitates hydrogen bonding and halogen interaction to some important amino residues which were responsible for antimalarial activity. Some important amino acid residue in binding to the WR99210 inhibitor appeared in the interaction of new compounds. They were Ile14, Cys15, Asp54, Ile164, Phe116, and Lys49. The resemblance of the interaction of new compounds to amino acid residues proved that new compounds have good antimalarial activities. Compound 22b was proposed as the best antimalarial compound. Figure 4 depicts that compound 22b could interact with amino acid residue Ile14, Asp54, and Ile164 through the hydrogen-bonding interactions. The hydrogen-bonding distance to the amino acid residue was found to be smaller. In addition, we also found that the presence of pyrrolidine at the C3 pyrimidine ring contributed to the hydrophobic interaction with the amino acid residue of Phe116. Of course, it produced a good impact on increasing the stability of the bond between the ligand compound (compound 22b) and the targeted protein, with a binding energy value of -8.9 kcal/mol. In addition, this binding energy has similar binding energy to WR99210 (-8.9 kcal/mol) and is proposed to be a suggested compound as an antimalarial candidate. Based on molecular docking results, the new design of the pyrimidine compound had good antimalarial activity. It proved that the new compound was able to interfere with folate biosynthesis in plasmodia. This was facilitated by the inhibition of the activity of *Plasmodium falciparum* dihydrofolate reductase-thymidylate synthase, thereby reducing the levels of tetrahydrofolate. Thus, the DNA replication disruption occurred [21].

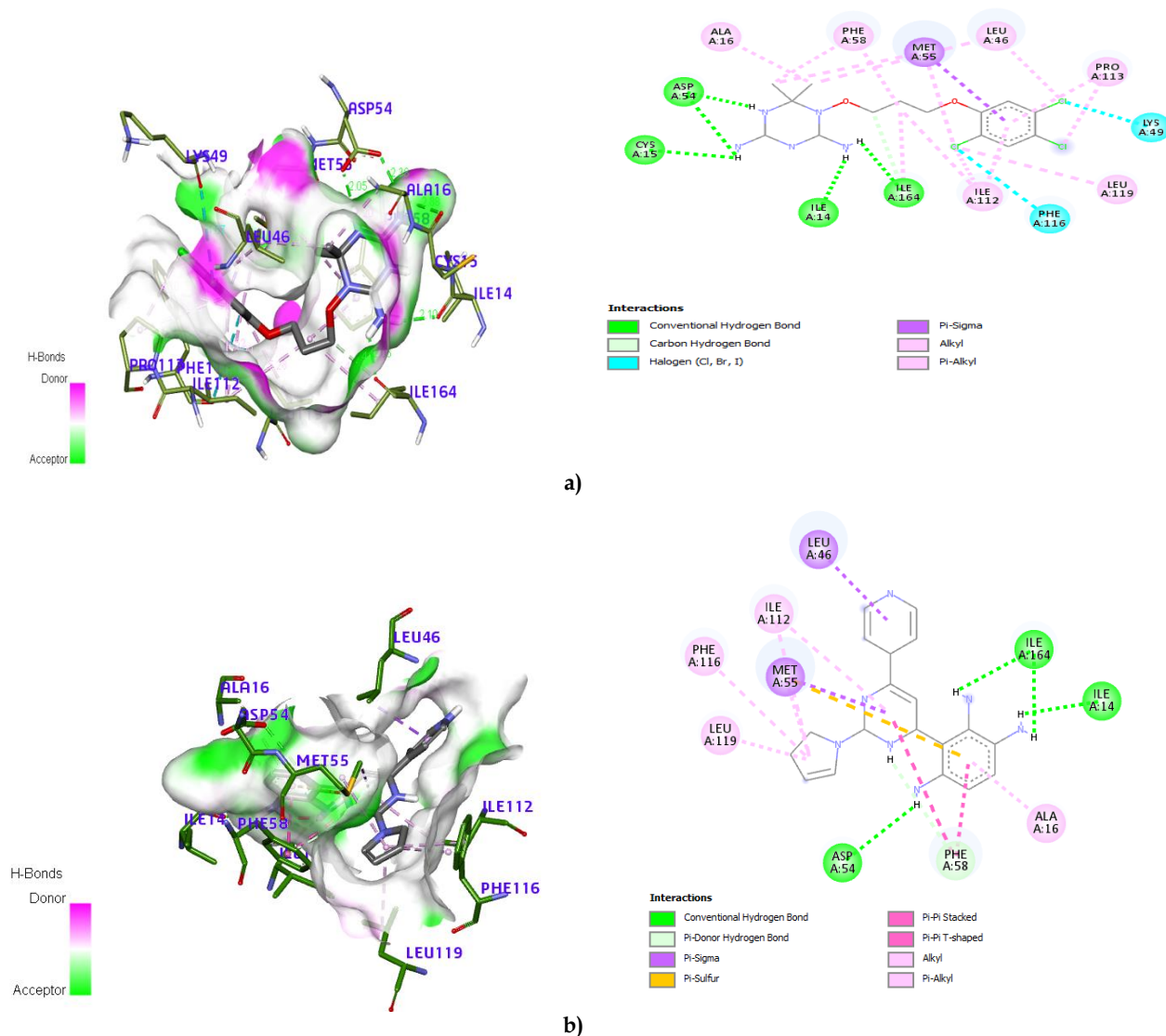


Figure 4. 2D and 3D interaction from the new design of pyrimidine compound on the active site of the *PfDHFR-TS* protein (ID: 1j3i). Ligand native WR99210 (a), and compound 22b (b).

3. CONCLUSION

QSAR analysis obtained the best equation model used as a guide for the design of new compounds, which was $\text{Log pMIC} = 10,441 - 16,769 (\text{qC7}) - 15,880 (\text{qC9}) + 5,809 (\text{qC12}) + 10,612 (\text{qC13}) + 114,506 (\text{LUMO})$. The new design of the pyrimidine compounds had a good antimalarial activity with the insertion of donating groups such as hydroxyl, amino, and *N,N*-dimethyl amine. The addition of the halogen group caused an increase in pMIC, where the best pMIC value was in the Iodo group. Molecular docking of the new compound proved the interaction between the new compound and several essential amino acid residues in the inhibition of *Plasmodium falciparum* dihydrofolate reductase-thymidylate synthase. Compound 22b, which was substituted for an amino group and a pyrrolidine group at the C3 position of its pyrimidine ring, gave the best docking score of -8.9 (kcal/mol).

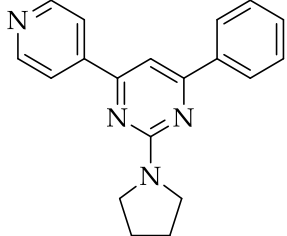
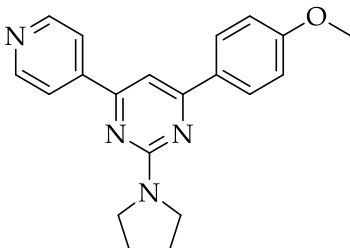
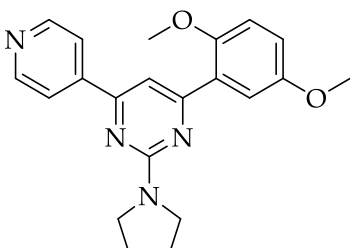
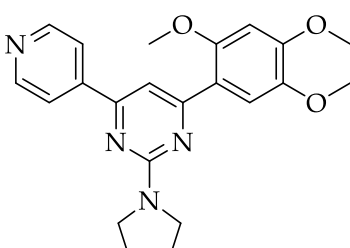
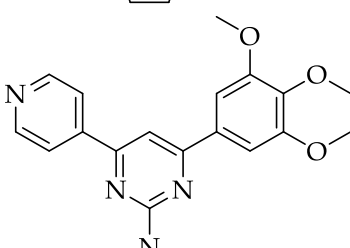
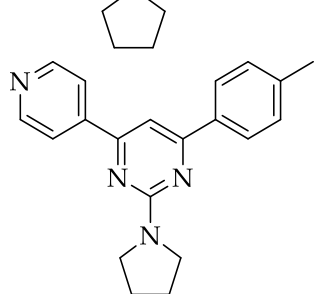
4. MATERIALS AND METHODS

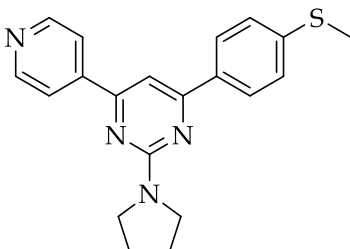
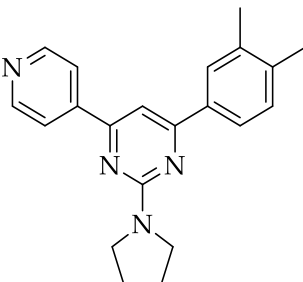
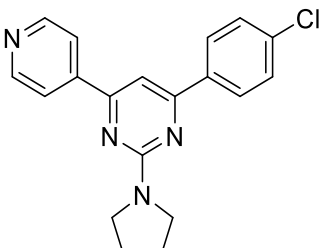
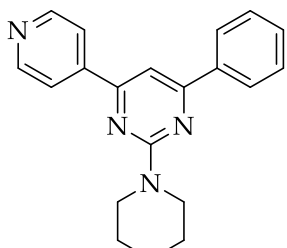
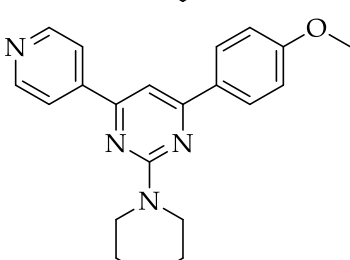
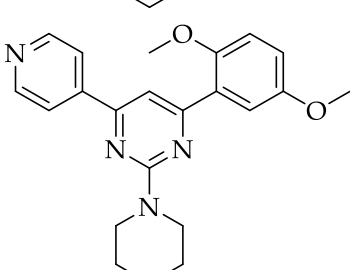
4.1. Data Set Analysis

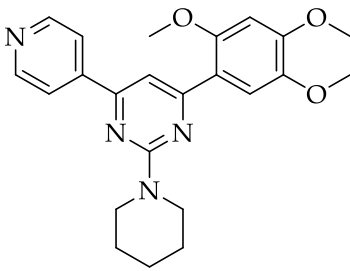
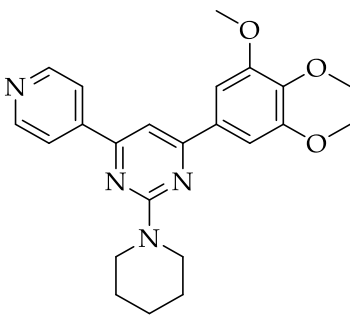
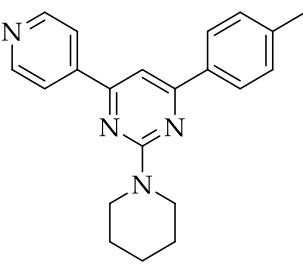
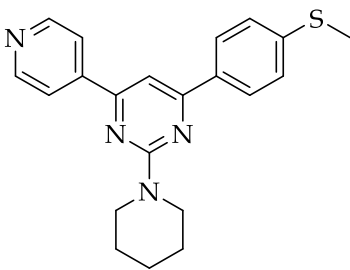
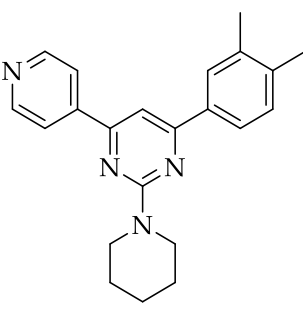
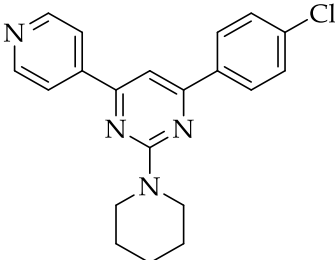
Pyrimidine derivatives compounds were taken from research data conducted by Agarwal et al. [7]. The 2,4,6-trisubstituted pyrimidine compounds along with antimalarial activity data (MIC, $\mu\text{g/mL}$) are shown in Table 6. Antimalarial activity data in MIC values, g/mL units were first converted to μM and then converted to pMIC values. The whole compounds are further divided into two parts, namely the training set

and the test set. The training set is used as data to build the QSAR equation, while the test set is used to validate the obtained QSAR equation.

Table 6. Antimalarial activity of 2,4,6-trisubstituted pyrimidine derivative compounds [7].

Compound id	Compound	pMIC
1		8.179
2		8.220
3*		8.559
4		8.593
5*		6.895
6		8.199

7		8.241
8		8.218
9*		8.225
10		8.199
11		8.238
12		8.274

13		8.609
14		6.910
15		9.121
16		8.258
17*		7.537
18		7.544

*test set compound

4.2. Instrumentation

This study used a laptop with specifications: Intel® Core™ i3-7020U CPU @ 2.3 GHz, 4 GB (RAM), Windows 10. Softwares installed were ChemDraw Professional 16, Chem 3D 16, Gaussian 09, SPSS statistic 25, CHIMERA 1.13, AutoDock Vina, AutoDock Tools 1.5.6, PyMOL, Discovery Studio Client 2021 Client®.

4.3. QSAR Analysis

The selection of the best computational method for optimization was carried out by analysing the chemical shift on compound 15. Compound 15 is chosen which has a high yield and purity. The Austin Model 1 (AM1), Parameterized Model Number 3 (PM3), Hartree-Fock (HF), and Density Functional Theory (DFT) were computational methods to determine ¹³C-NMR chemical shift analysis using Gaussian 09. The best computational model was determined from the PRESS value by adding up the difference between the experimental value and the predicted value. The smallest PRESS value indicates the best model which was then used for compound optimization. The optimized training set compounds would determine the charge value, HOMO, and LUMO as electronic descriptors. This descriptor was then analysed statistically using SPSS software with the Multi Linear Regression Backward method to build the QSAR equation. The selected data set was used to validate the existing QSAR equation.

4.4. Statistical Analysis

The best QSAR equation model was selected based on statistical analysis including the values of R, R², adjusted R², standard estimation of error (SEE), F_{cal}/F_{table}, and PRESS (predictive residual sum of the square). The selected QSAR equation model was then validated on the data set. The R² value greater than 0.6 [18] and the smallest PREES value were considered to be used for the design of new compounds [17].

4.5. Design of The New Compounds

Modification of the 2,4,6-trisubstituted pyrimidine was performed by adding the new substitute on the active side that was responsible for antimalarial activity. The chemistry insight is the guidance to modify the structure to consider the relationship between structure and biological activity. The compound with the highest pMIC value (Table 1) was used as the basis for obtaining new compounds with better antimalarial activity. The high pMIC value (low MIC) indicated that the substitute introduced in the new compound had a major influence on antimalarial activity.

4.6. Molecular Docking

Ligand preparation. Molecular docking was carried out for the best compounds obtained from the QSAR analysis to determine the interaction with the targeted protein. The new compound design was created in 2D using ChemDraw Professional 16 and converted into a 3D structure in Chem 3D 16. All 3D compounds were geometrically optimized using Gaussian 09 software with the AM1 method.

Targeted protein preparation. The protein structure was retrieved from the Protein Data Bank database with PDB ID: 1J31. The molecule water was removed from protein using chimera 1.13 and added all hydrogen along with Kollman charge using AutoDock tools 1.5.6. Further, the addition of hydrogen atoms and Gasteiger charge was also performed. In the docking analysis, the docking grid was on the active side of PfDHFR-TS protein with grid box sizes for center x, y, z respectively 12 x 14 x 12 Armstrong and the space value of 1 Armstrong. 2D and 3D Visualization of the docking results used Discovery Studio Client 2021 Client®. The docking protocol validation was to the WR99210 as a native ligand. The root-mean-square deviation (RMSD) value of the native docking ligand met the requirements of below 2 Armstrong [22]. RMSD value was analyzed using PyMOL.

Author contributions: Concept – P.J.P.T.; Design – P.J.P.T.; Supervision – F.O.N., D.M.; Resources – P.J.P.T.; Materials – P.J.P.T.; Data Collection and/or Processing – P.J.P.T.; Analysis and/or Interpretation – P.J.P.T., F.O.N. D.M.; Literature Search – P.J.P.T., F.O.N. D.M.; Writing – P.J.P.T.; Critical Reviews – P.J.P.T., F.O.N., D.M.

Conflict of interest statement: The authors declared that there is no conflict of interest in the manuscript.

REFERENCES

- [1] White N, Dondrop A. Malaria. In: Firth J, Conlon C, Cox T (eds) Oxford Textbook of Medicine. Oxford University Press, London, 2020, pp. 1395–1414.

- [2] WHO, Malaria, https://www.who.int/health-topics/malaria#tab=tab_1 (accessed October 18, 2021).
- [3] Guntur RD, Kingsley J, Islam FMA. Epidemiology of Malaria in East Nusa Tenggara Province in Indonesia: Protocol for a Cross-sectional Study. *JMIR Res Protoc*. 2021; 10(4): 1–36. [CrossRef]
- [4] Jiero S, Pasaribu AP. Haematological profile of children with malaria in Sorong, West Papua, Indonesia. *Malar J*. 2021; 20(1): 1–12. [CrossRef]
- [5] Pradines B. Antimalarial Drug Resistance: Clinical Perspectives. In: Mayers D., Sobel J., Ouellette M, et al. (eds) *Antimicrobial Drug Resistance*. Springer International Publishing AG, Switzerland, 2017, pp. 1245–1275.
- [6] Kalaria K., Karad S., Raval D. A review on diverse heterocyclic compounds as the privileged scaffolds in antimalarial drug discovery. *Eur J Med Chem*. 2018; 158: 917–936. [CrossRef]
- [7] Agarwal A, Srivastava K, Puri SK, Chauhan PMS. Synthesis of 2,4,6-trisubstituted pyrimidines as antimalarial agents. *Bioorganic Med Chem*. 2005; 13(15): 4645–4650. [CrossRef]
- [8] Cabrera DG, Douelle F, Manach CL, Han Z, Paquet T, Taylor D, Njoroge M, Lawrence N, Wiesner L, Witty MJ, Wittlin S, Street LJ, Chibale K. Structure Activity Relationship Studies of Orally Active Antimalarial 3,5-Substituted 2-Aminopyridines. *J Med Chem*. 2012; 55(24): 11022–11030. [CrossRef]
- [9] Pal K, Raza MK, Legac J, Rahman MA, Manzoor S, Rosenthal PJ, Hoda N. Design, synthesis, crystal structure and anti-plasmodial evaluation of tetrahydrobenzo[4,5]thieno[2,3-d]pyrimidine derivatives. *RSC Med Chem*. 2021; 12: 970–981. [CrossRef]
- [10] Manohar S, Rajesh UC, Khan SI, Tekwani BL, Rawat DS. Novel 4-aminoquinoline-pyrimidine based hybrids with improved in vitro and in vivo antimalarial activity. *ACS Med Chem Lett*. 2012; 3(7): 555–559. [CrossRef]
- [11] Asif M. Green Synthesis, Green Chemistry, and Environmental Sustainability: An Overview on Recent and Future Perspectives Green Chemistry in Pharmaceuticals. *Green Chem Technol Lett*. 2021; 7(1): 18–27. [CrossRef]
- [12] Surabhi, Singh B. Computer aided drug design. *J Drug Deliv Ther Open*. 2018; 8(5): 504–509. [CrossRef]
- [13] Jufrizal S, Purnomo B, Armunanto R. Design of New Potential Antimalaria Compound Based on QSAR Analysis of Chalcone Derivatives. *Int J Pharm Sci*. 2016; 36(2): 71–76.
- [14] Chaianantakul N, Sirawaraporn R, Sirawaraporn W. Insights Into The Role of The Junctional Region of *Plasmodium falciparum* Dihydrofolate Reductase-Thymidylate Synthase. *Malar J*. 2013; 12(91): 1–13. [CrossRef]
- [15] Mishra R, Mishra B, Moorthy NSHN. Dihydrofolate Reductase Enzyme: A Potent Target for Antimalarial Research. *Asian J Cell Biol*. 2006; 1(1): 48–58. [CrossRef]
- [16] Syahri J, Yuanita E, Nurohmah BA. Xanthone as Antimalarial : QSAR Analysis, Synthesis, Molecular Docking and In-vitro Antimalarial Evaluation. *Orient J Chem*. 2017; 33(1): 29–40. [CrossRef]
- [17] Frimayanti N, Yam ML, Lee HB, Othman R, Zain SM, Rahman NA. Validation of quantitative structure-activity relationship (QSAR) model for photosensitizer activity prediction. *International Journal of Molecular Sciences*. 2011; 12(12): 8626–8644. [CrossRef]
- [18] Golbraikh A, Shen M, Xiao Z, Xiao YD, Lee KH, Tropsha A. Rational Selection of Training and Test Sets For The Development of Validated QSAR Models. *J Comput Aided Mol Des*. 2003; 17: 241–253. [CrossRef]
- [19] Padmaja L, Ravikumar C, Sajan D, Joe IH, Jayakumar VS, Pettit GR, Nielsen OF. Density functional study on the structural conformations and intramolecular charge transfer from the vibrational spectra of the anticancer drug combretastatin-A2. *J Raman Spectrosc*. 2009; 40(4): 419–428. [CrossRef]
- [20] Miar M, Shiroudi A, Pourshamsian K, Oliay AR, Hatamjafari F. Theoretical investigations on the HOMO-LUMO gap and global reactivity descriptor studies, natural bond orbital, and nucleus-independent chemical shifts analyses of 3-phenylbenzo[d]thiazole-2(3H)-imine and its para-substituted derivatives: Solvent and substituent effects. *J Chem Res*. 2021; 45: 147–158. [CrossRef]
- [21] Gregson A, Plowe C. Mechanisms of Resistance of Malaria Parasites to Antifolates. *Pharmacol Rev*. 2005; 57(1): 117–145. [CrossRef]
- [22] Hadni H, Elhallaoui M. 2D and 3D-QSAR, Molecular Docking and ADMET Properties: In Silico Studies of Azaaurones As Antimalarial Agents. *New J Chem*. 2020; 44(16): 6553–6565. [CrossRef]